

Stereochemistry of linking segments in the design of helix–helix motifs in peptides. Crystallographic comparison of a glycyldipropylglycyl–glycyl segment in a tripeptide and a 14-residue peptide



Saumen Datta,^a Ramesh Kaul,^{b,c} R. Balaji Rao,^c N. Shamala^{*,a} and P. Balaram^{*,b}

^a Department of Physics, Indian Institute of Science, Bangalore-560012, India

^b Molecular Biophysics Unit, Indian Institute of Science, Bangalore-560012, India

^c Department of Chemistry, Banaras Hindu University, Varanasi-221005, India

As part of a program to develop synthetic helix–linker–helix peptides the conformational properties of various linking segments are currently being investigated. The propensity of α,α -di-*n*-propylglycine (Dpg) residues to adopt backbone conformations in the extended region of the Ramachandran map, suggested by theoretical calculations and supported by experimental observations, prompted us to investigate the utility of the Gly-Dpg-Gly segment as a rigid linking motif. The crystal structure of the achiral tripeptide Boc-Gly-Dpg-Gly-OH **1** revealed a fully extended conformation ($\varphi = \pm 178^\circ$, $\psi = \pm 171^\circ$) at Dpg(2), with Gly(1) adopting a helical conformation ($\varphi = \mp 72^\circ$, $\psi = \mp 32^\circ$). The addition of flanking helical segments in the 14 residue peptide Boc-Val-Val-Ala-Leu-Gly-Dpg-Gly-Val-Ala-Leu-Aib-Val-Ala-Leu-OMe **2** resulted in the crystallographic characterization of a continuous helix over the entire length of the peptide. Peptide **1** crystallized in the centrosymmetric space group $P2_1/c$ with $a = 9.505(2)$ Å, $b = 11.025(2)$ Å, $c = 20.075(4)$ Å, $\beta = 90.19^\circ$ and $Z = 4$. Peptide **2** crystallized in space group $P2_12_12_1$ with $a = 10.172(1)$ Å, $b = 17.521(4)$ Å, $c = 46.438(12)$ Å and $Z = 4$. A comparative analysis of Gly-Dpg-Gly segments from available crystal structures indicates a high conformational variability of this segment. This analysis suggests that context and environment may be strong conformational determinants for the Gly-Dpg-Gly segment.

Introduction

The ability to construct stereochemically well-defined peptide helices, using α -aminoisobutyric acid (Aib) and related α,α -dialkylated glycines,^{1–6} has stimulated attempts to assemble helix–linker–helix motifs as models for super secondary structures in proteins.⁷ The use of nonhelical linkers should facilitate the design of molecules with distinct helical segments. A close packed, approximately antiparallel helix arrangement may then be achieved as a consequence of solvophobic effects, in which release of solvent molecules entropically drives the association of large complementary molecular surfaces.^{8–10} In the ‘Mecano set’ approach being developed in this laboratory, various linking segments are being investigated. Earlier reports have

described attempts to use Gly-Pro units,¹¹ D-amino acids¹² and ϵ -aminocaproic acid (Acp)¹³ as linking units between helix pairs. In this paper we describe an analysis of the linking segment Gly-Dpg-Gly (Dpg = α,α -di-*n*-propylglycine). The choice of Dpg was stimulated by a report that higher α,α -di-*n*-alkylglycines have pronounced energy minima in the fully extended (φ , $\psi \approx 180^\circ$) region of conformational space,^{14,15} suggesting the utility of this residue in designing stereochemically rigid nonhelical segments. Interestingly, while early crystal structure analyses of homo-oligopeptides containing Dpg provided evidence for the occurrence of the fully extended conformations,^{16,17} many subsequent reports provided examples of Dpg in helical conformations.^{6,18} Both theoretical and experimental studies suggest that two distinct regions of conformational

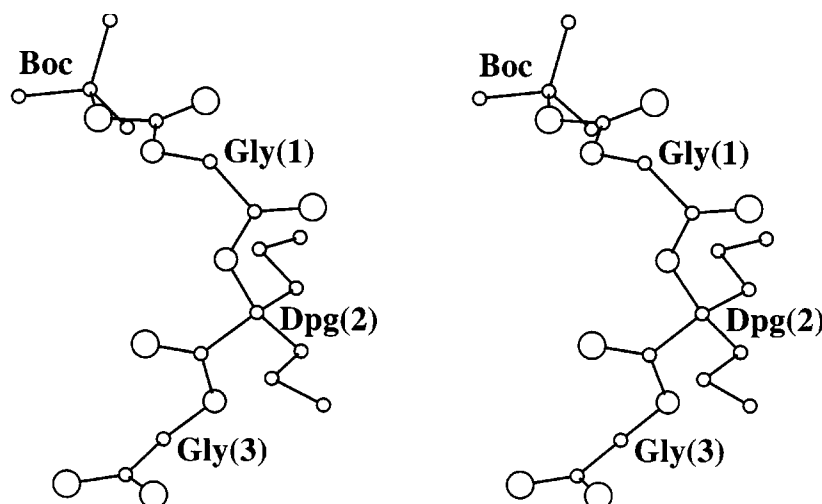


Fig. 1 A stereoview of the tripeptide Boc-Gly-Dpg-Gly-OH **1** structure

Table 1 Crystal data and structure refinement details for peptide **1** and **2**

	Peptide 1	Peptide 2
Empirical formula	C ₁₇ H ₃₁ N ₃ O ₆	C ₇₀ H ₁₂₄ N ₁₄ O ₁₉
Formula weight	373.45	1465.83
Temperature	293(2) K	293(2) K
Wavelength	1.541 80 Å	1.541 80 Å
Crystal system	Monoclinic	Orthorhombic
Space group	<i>P</i> 2 ₁ / <i>c</i>	<i>P</i> 2 ₁ 2 ₁ 2 ₁
Unit cell dimensions	<i>a</i> = 9.505(2) Å <i>b</i> = 11.025(2) Å <i>c</i> = 20.075(4) Å <i>a</i> = 90° <i>β</i> = 90.19° <i>γ</i> = 90°	<i>a</i> = 10.172(1) Å <i>b</i> = 17.521(4) Å <i>c</i> = 46.438(12) Å <i>a</i> = 90° <i>β</i> = 90° <i>γ</i> = 90°
Volume	2103.7(7) Å ³	8276(3) Å ³
<i>Z</i>	4	4
Density (calculated)	1.179 Mg m ⁻³	1.176 Mg m ⁻³
Absorption coefficient	0.740 mm ⁻¹	0.704 mm ⁻¹
<i>F</i> (000)	808	3176
Crystal size	0.4 × 0.4 × 0.4 mm	0.8 × 0.5 × 0.2 mm
<i>θ</i> range for data collection	4.40–74.98°	1.90–75.21°
Index ranges	−11 ≤ <i>h</i> ≤ 11 0 ≤ <i>k</i> ≤ 13 0 ≤ <i>l</i> ≤ 25	0 ≤ <i>h</i> ≤ 12 0 ≤ <i>k</i> ≤ 21 0 ≤ <i>l</i> ≤ 58
Independent reflections	4323	9428
Reflections [<i>I</i> > 2σ(<i>I</i>)]	3409	7231
Data/restraints/parameters	4323/0/265	9428/0/1052
Goodness-of-fit	0.959	1.312
Final <i>R</i> indices [<i>I</i> > 2σ(<i>I</i>)]	<i>R</i> ₁ = 0.0460 <i>wR</i> ₂ = 0.1350	<i>R</i> ₁ = 0.0557 <i>wR</i> ₂ = 0.1569
<i>R</i> indices (all data)	<i>R</i> ₁ = 0.0572 <i>wR</i> ₂ = 0.1468	<i>R</i> ₁ = 0.0711 <i>wR</i> ₂ = 0.1671
Largest difference peak and hole	0.242 and −0.288 e Å ⁻³	0.468 and −0.240 e Å ⁻³

Table 2 Backbone dihedral angles for the Gly-Dpg-Gly segment in peptide crystal structures

Residue	Dihedral angles/° ^a	Segment 1 ^b	Segment 2 ^c	Segment 3 ^d	Segment 4 ^e	Segment 5
Gly	<i>φ</i>	−72	−66	−94, −96 ^f	72	−80
	<i>ψ</i>	−32	−51	−162, −153	−166	−18
Dpg ^g	<i>φ</i>	178	−52	−53, −56	−54	56
	<i>ψ</i>	171	−44	−50, −47	−46	32
Gly	<i>φ</i>	−63	−63	−64, −65	−78	85
	<i>ψ</i>		−34	−36, −40	−9	−3

^a Dihedral angle nomenclature follows that described in ref. 29. ^b Boc-Gly-Dpg-Gly-OH (this study). ^c Boc-Val-Val-Ala-Leu-Gly-Dpg-Gly-Val-Ala-Leu-Aib-Val-Ala-Leu-OMe (this study). ^d Boc-Gly-Dpg-Gly-Val-Ala-Leu-Aib-Val-Ala-Leu-OMe (ref. 27). ^e Boc-Gly-Dpg-Gly-Gly-Dpg-Gly-NHMe. Segment 4 is the N-terminus tripeptide and segment 5 corresponds to the C-terminus tripeptide (ref. 28). ^f Two values correspond to the two conformers present in the crystallographic asymmetric unit. ^g The Dpg sidechain torsion angles in peptide **1** (this study) are *χ*¹ (−57°, 56°), *χ*² (170°, 170°).

space (fully extended and helical) are energetically accessible to Dpg residues. The sequence context and environmental influences presumably determine the precise nature of the conformation adopted. The use of Gly-Dpg-Gly in the present study was dictated by the fact that Gly is highly conformationally flexible and has a relatively low helix propensity. We describe in this report crystal structures of a tripeptide Boc-Gly-Dpg-Gly-OH (peptide **1**) and a 14 residue peptide Boc-Val-Val-Ala-Leu-Gly-Dpg-Gly-Val-Ala-Leu-Aib-Val-Ala-Leu-OMe (peptide **2**). While the Dpg residue adopts a fully extended conformation in the former, a continuous helix is obtained in the latter. Comparisons with other crystallographically determined Gly-Dpg-Gly segments reveals a significant degree of conformational variability in the sequence.

Experimental

Peptides were synthesized by conventional solution phase procedures¹⁹ and purified by medium pressure liquid chromatography on a reverse phase C₁₈ (40–60 μ) column using methanol–water gradients. Peptides were checked for homogeneity by high performance liquid chromatography on a

Table 3 Torsion Angles^a (°) in Boc-Val-Val-Ala-Leu-Gly-Dpg-Gly-Val-Ala-Leu-Aib-Val-Ala-Leu-OMe (peptide **2**)

Residue	<i>φ</i>	<i>ψ</i>	<i>ω</i>	<i>χ</i> ¹	<i>χ</i> ²
Val (1)	−61 ^b	−23	175	−64, 63	
Val (2)	−55	−42	180	−70, 167	
Ala (3)	−61	−38	179		
Leu (4)	−68	−39	180	−60	−64, 173
Gly (5)	−66	−51	173		
Dpg (6)	−52	−44	−176	−69, 170	178, −178
Gly (7)	−63	−34	177		
Val (8)	−63	−45	178	−68, 167	
Ala (9)	−62	−40	176		
Leu (10)	−60	−51	−169	176	66, −171
Aib (11)	−56	−44	−172		
Val (12)	−78	−10	−178	67, −59	
Ala (13)	−106	−6	−179		
Leu (14)	−94	177 ^c	−176 ^d	−77	−50, −178

^a The torsion angles for rotation about bonds of the peptide backbone (*φ*, *ψ*, and *ω*) and about bonds of the amino acid side-chains (*χ*¹, *χ*²) as suggested by the IUPAC-IUB Commission on Biochemical Nomenclature (ref. 29). Estimated standard deviations ~1.0°. ^b C'(0)–N(1)–C^α(1)–C'(1). ^c N(14)–C^α(14)–C'(14)–O(OMe). ^d C^α(14)–C'(14)–O(OMe)–C(OMe).

Table 4 Potential hydrogen bond parameters in Boc-Val-Val-Ala-Leu-Gly-Dpg-Gly-Val-Ala-Leu-Aib-Val-Ala-Leu-OMe

Type	Donor	Acceptor	Bond length/Å		Bond angle/°		
			N...O	H...O	C=O...H	C=O...N	O...HN
Intermolecular	O(W)	O(13)	2.83				
	N(1)	O(W) ^a	3.14				
	N(2)	O(W) ^a	3.04				
Intramolecular							
4 → 1 ^b	N(3)	O(0)	3.01	2.33	123	130	137
4 → 1 ^b	N(4)	O(1)	3.01	2.50	100	114	119
4 → 1	N(5)	O(2)	3.20	2.71	92	105	117
4 → 1	N(6)	O(3)	3.76	3.51	85	97	100
4 → 1	N(7)	O(4)	3.19	2.81	84	99	109
4 → 1 ^c	N(8)	O(5)	3.18	2.57	100	111	129
4 → 1	N(9)	O(6)	3.23	2.78	104	116	114
4 → 1	N(10)	O(7)	3.35	2.98	86	99	109
4 → 1	N(11)	O(8)	3.32	2.84	91	103	117
4 → 1	N(12)	O(9)	3.70	3.11	96	105	128
4 → 1 ^b	N(13)	O(10)	3.02	2.23	112	121	152
4 → 1	N(14)	O(11)	3.54	2.71	102	106	163
5 → 1	N(4)	O(0)	3.79	3.00	141	141	155
5 → 1 ^b	N(5)	O(1)	2.96	2.16	157	164	156
5 → 1 ^b	N(6)	O(2)	3.0	2.20	161	160	172
5 → 1 ^b	N(7)	O(3)	2.94	2.19	132	142	145
5 → 1 ^b	N(8)	O(4)	2.92	2.20	146	153	143
5 → 1 ^c	N(9)	O(5)	3.48	2.63	153	155	167
5 → 1 ^b	N(10)	O(6)	3.04	2.21	156	160	164
5 → 1 ^b	N(11)	O(7)	2.86	2.06	146	152	154
5 → 1 ^c	N(12)	O(8)	3.38	2.57	149	152	158
5 → 1	N(13)	O(9)	3.67	3.12	135	145	124
5 → 1 ^c	N(14)	O(10)	3.20	2.69	135	169	119
Solvent-peptide	O(M) ^d	O(3)	2.88				

^a Symmetrically related by the relation $(-x + \frac{1}{2}, -y + 1, z + \frac{1}{2})$. ^b These are the acceptable hydrogen bonds satisfying the criteria of hydrogen bond geometry (ref. 24). ^c These are the weak hydrogen bonds (ref. 24). ^d Oxygen atom of CH₃OH.

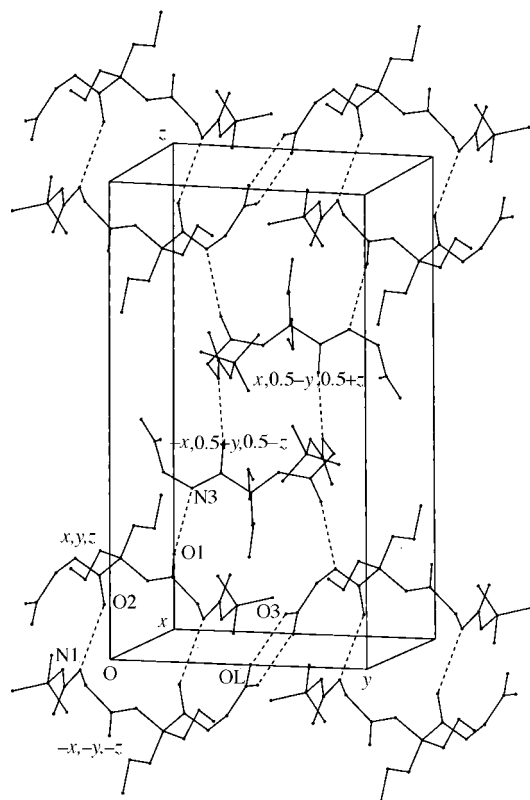


Fig. 2 Packing diagram for Boc-Gly-Dpg-Gly-OH **1**. The intermolecular hydrogen bonds [O(1)···N(3)[$-x, 0.5 + y, 0.5 - z$] = 2.84 Å, O(2)···N(1)[$-x + 1, -y, -z$] = 2.98 Å, O(3)···O(L)[$-x + 1, -y + 1, -z$] = 2.62 Å] are indicated by broken lines.

reversed phase C₁₈ (5 μ) column and characterized by 400 MHz ¹H NMR spectroscopy. Peptide **2** was obtained as a deletion sequence in the synthesis of a longer symmetrical seventeen residue peptide.

Crystals of peptide **1** and **2** were obtained by slow evaporation from a methanol-water solution. X-Ray diffraction data for both the peptide crystals were collected at room temperature, 21 °C, with an automated four-circle diffractometer using Cu-K_α ($\lambda = 1.5418$ Å) radiation. 25 reflections in the $10^\circ \leq \theta \leq 15^\circ$ range were used for determining the cell constants in both cases. Though the β value (90.19°) is close to 90° in the case of peptide **1**, the significant difference between hkl and the corresponding $\bar{h}k\bar{l}$ reflections suggests a monoclinic cell. In the case of peptide **1** the structure was determined by the direct phase determination method.²⁰ The structure of peptide **2** was obtained by the vector search method²¹ followed by partial structure expansion.²² The helical backbone fragment (residue 2 to residue 8) of the sequence Boc-Aib-Val-Ala-Leu-Aib-Val-Ala-Leu-Aib-OMe²³ was used in the search method. Both the peptide structures were refined isotropically followed by anisotropic least-squares refinement. Hydrogen atoms were added geometrically and allowed to ride with the corresponding heavy atoms in the final cycle of the refinement. All the relevant crystallographic data collection parameters and structure refinement details for the two peptides are summarized in Table 1.†

† Atomic coordinates, bond lengths and angles, and thermal parameters have been deposited at the Cambridge Crystallographic Data Centre (CCDC). For details of the deposition scheme, see 'Instructions for Authors', *J. Chem. Soc., Perkin Trans. 2*, 1997, Issue 1. Any request to the CCDC for this material should quote the full literature citation and the reference number 188/80.

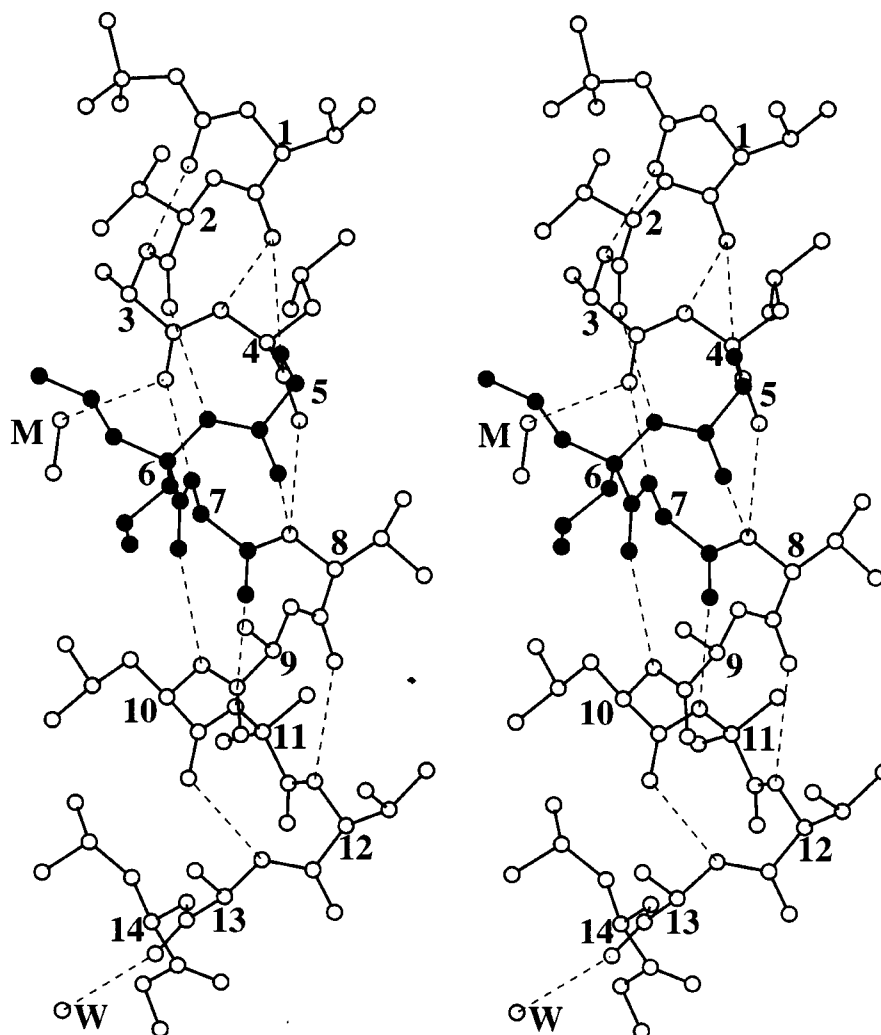


Fig. 3 Stereoview of the crystal structure of peptide **2**. The Gly-Dpg-Gly segment is indicated in bold type. The intramolecular hydrogen bonds are indicated by broken lines (see Table 4).

Results and discussion

Extended Dpg residue in peptide 1

Fig. 1 shows a stereoview of the molecular conformation of tripeptide **1** in crystals. The backbone conformational angles are listed in Table 2, which also provides a comparison with structures of the same segment in larger peptides. In tripeptide **1** the Dpg residue adopts a fully extended conformation while Gly(1) lies in the helical region. The achiral peptide crystallizes in a centrosymmetric space group, with molecules of both helical senses being present in the unit cell. The molecules are held in the crystal by intermolecular hydrogen bonds formed between symmetry related molecules (Fig. 2). Surprisingly, several hydrogen bond donor and acceptor groups do not participate in hydrogen bonding interactions.

The peptide helix in the 14 residue peptide 2

Fig. 3 shows a stereoview of the conformation of the 14 residue peptide determined in crystals. The backbone and side-chain torsion angles are listed in Table 3. Intramolecular and intermolecular hydrogen bonds are summarized in Table 4. Hydrogen bond parameters are listed for all potential $4 \rightarrow 1$ and $5 \rightarrow 1$ interactions to provide a ready assessment of helix type. This assumes importance in view of the fact that in helical peptides assignment of 3_{10} and α -helical structures is not always readily apparent.²⁴ The molecule forms an almost completely α -helical structure, stabilized by successive $5 \rightarrow 1$ hydrogen bonds. As frequently observed in peptide helices there is a 3_{10} -helical turn at the N-terminus with a $4 \rightarrow 1$ hydrogen bond

between the Boc(0)CO and Ala(3)NH groups. A single 3_{10} -helical hydrogen bond is also observed near the C-terminus between Leu(10)CO and Ala(13)NH groups. In the centre of the helix there is a evidence of a possible transition between α and 3_{10} -helical structures. Gly(5)CO appears to be involved in a $4 \rightarrow 1$ interaction with Val(8)NH, while a corresponding $5 \rightarrow 1$ interaction with Ala(9)NH is definitely weaker as indicated by the $N \cdots O$ distances. The molecules pack in the crystal as columns of antiparallel helices, held together in each column by head-to-tail hydrogen bonds mediated by a single bridging water molecule (Fig. 4). A lone methanol molecule is trapped between helical columns and forms a single hydrogen bond with the CO group of Ala(3). This is a relatively rare example of solvation involving bifurcated hydrogen bond formation to a CO group involved in a strong intrahelical hydrogen bond. Such solvent interactions are also observed in protein structures.²⁵ The CH_3 group of the CH_3OH molecule is in close van der Waals contact with the hydrophobic side chains of Ala(3), Dpg(6), Leu(4) $[-1 + x, y, z]$, Val(8) $[-1 + x, y, z]$, and Aib(9) $[1 - x, \frac{1}{2} + y, \frac{1}{2} - z]$ residues (Fig. 5). Such trapped alcohol molecules in helical clusters have also been observed earlier in structures of hydrophobic helices.²⁶

Context dependent Gly-Dpg-Gly conformation

Fig. 6 shows an overlay of the structures of the 14 residue peptide **2** and the helical decapeptide Boc-Gly-Dpg-Gly-Val-Ala-Leu-Aib-Val-Ala-Leu-OMe.²⁷ Residues 5–14 of peptide **2** are exactly identical in sequence to the decapeptide. Comparison of the dihedral angles in Table 2 together with Fig. 6

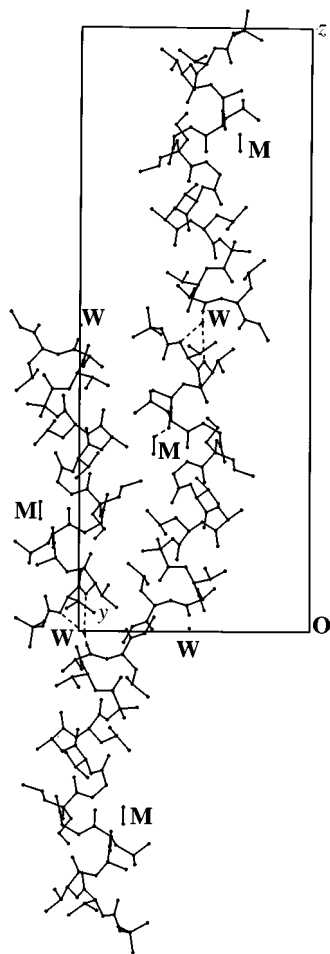


Fig. 4 Packing diagram for the 14-residue peptide **2**. View down the crystallographic x -axis. Intermolecular hydrogen bonds are indicated by broken lines. W indicates the oxygen molecule of the water and M represents the trapped methanol molecule.

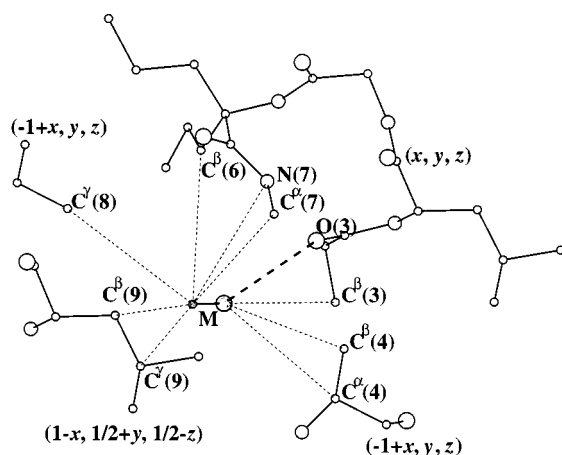


Fig. 5 The van der Waals environment of the methanol molecule (M). Atoms which lie within ~ 4 Å are indicated by the dotted lines. The bold broken line indicates the hydrogen bond between the oxygen atom of methanol and the Ala(3)CO group.

establishes that the Gly-Dpg-Gly segment switches to a completely helical conformation in peptide **2**, whereas a nonhelical N-terminus is observed in the decapeptide. Interestingly, Table 2 shows that the 14 residue peptide **2** is the only example where the Gly-Dpg-Gly segment adopts a completely helical conformation. In four out of five peptides listed in Table 2 the Dpg residue adopts helical ϕ , ψ values, with peptide **1** being the sole exception. However, the overall conformation of the tripeptide segment is nonhelical in all the cases with the exception of peptide **2**. In two examples Gly(1) adopts a semi-extended con-

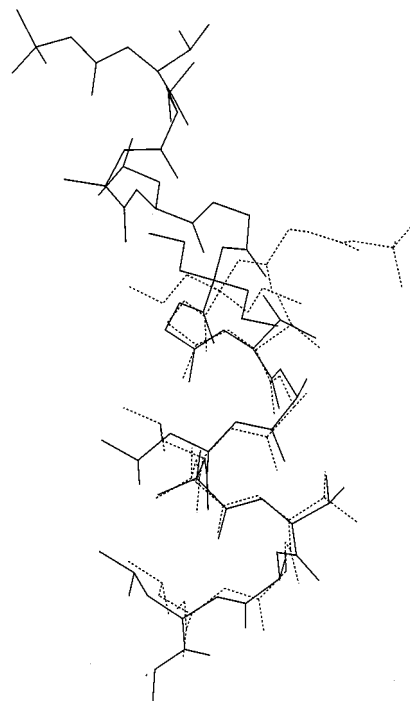


Fig. 6 Superposition of the structure of the 14-residue peptide (peptide **2**) and the decapeptide Boc-Gly-Dpg-Gly-Val-Ala-Leu-Aib-Val-Ala-Leu-OMe.²⁷ The former is indicated by the solid line, while the latter is represented by a broken line.

formation. The peptide Gly-Dpg-Gly-Gly-Dpg-Gly-NHMe provides an interesting example of a multiple β -turn structure. The N-terminus Gly-Dpg-Gly segment exhibits a type-II (II') β -turn conformation with Gly(1) and Dpg(2) occupying the $i + 1$ and $i + 2$ positions. The C-terminus Gly-Dpg-Gly segment forms a type-I (I') β -turn centred at Dpg(5) and Gly(6). While Gly(4) and Dpg(5) adopt helical ϕ , ψ values, the signs of the dihedral angles are opposite, indicative of opposing helix senses.²⁸

The above comparison of the Gly-Dpg-Gly conformation in peptides of varying length and sequence suggests that the conformation of this segment may be modulated by subtle environmental effects. Although Dpg residues are constrained to adopt helical or fully extended conformations, the combination of these two stereochemical alternatives with ϕ , ψ variations at the flanking Gly residues leads to appreciable conformational diversity. Somewhat disappointingly, the Gly-Dpg-Gly segment in the 14-residue peptide **2** favours a helical conformation, resulting in the characterization of a long cylindrical helix in crystals. The overwhelming crystallinity of hydrophobic helical peptide suggests that packing of apolar cylinders into crystalline lattices must be highly favourable. The extent to which the energetics of crystal packing promote the selection of helical conformations in peptide single crystals remains to be established. The present study reaffirms the necessity of interrupting intramolecular hydrogen bonding patterns in order to achieve helix termination in the middle of long hydrophobic sequences.

Acknowledgements

This research was supported by the Department of Science and Technology, Government of India. R. K. was supported by a Research Associateship of the Department of Biotechnology, Government of India.

References

- 1 I. L. Karle and P. Balam, *Biochemistry*, 1990, **29**, 6747.
- 2 P. Balam, *Curr. Opin. Struct. Biol.*, 1992, **2**, 845.

- 3 I. L. Karle, J. L. Flippen-Anderson, R. Gurunath and P. Balam, *Protein Sci.*, 1994, **4**, 1547.
- 4 A. Banerjee, S. Datta, A. Pramanik, N. Shamala and P. Balam, *J. Am. Chem. Soc.*, 1996, **118**, 9477.
- 5 I. L. Karle, R. B. Rao, S. Prasad, R. Kaul and P. Balam, *J. Am. Chem. Soc.*, 1994, **116**, 10 355.
- 6 I. L. Karle, R. Gurunath, S. Prasad, R. Kaul, R. B. Rao and P. Balam, *J. Am. Chem. Soc.*, 1995, **117**, 9632.
- 7 P. Balam, *Pure Appl. Chem.*, 1992, **64**, 1061.
- 8 J. A. Bryant, C. B. Knobler and D. J. Cram, *J. Am. Chem. Soc.*, 1990, **112**, 1254.
- 9 J. A. Bryant, J. L. Ericson and D. J. Cram, *J. Am. Chem. Soc.*, 1990, **112**, 1254.
- 10 G. M. Whitesides, E. E. Simanek, J. P. Mathias, C. T. Seto, D. N. Chin, M. Mammen and D. M. Gordon, *Acc. Chem. Res.*, 1995, **28**, 37.
- 11 K. Uma, I. L. Karle and P. Balam, in *Proteins: Structure Dynamics and Design*, eds. V. Renugopalakrishnan, P. R. Carey, I. C. P. Smith, S. G. Huang and A. Storer, ESCOM Science Publishers B. V., Leiden, 1991.
- 12 R. Gurunath and P. Balam, *Biochem. Biophys. Res. Commun.*, 1994, **202**, 241.
- 13 I. L. Karle, J. L. Flippen-Anderson, M. Sukumar, K. Uma and P. Balam, *J. Am. Chem. Soc.*, 1991, **113**, 3952.
- 14 E. Benedetti, C. Toniolo, P. M. Hardy, V. Barone, A. Bavoso, B. DiBlasio, P. Grimaldi, F. Lelj, V. Pavone, C. Pedone, G. M. Bonora and I. Lingham, *J. Am. Chem. Soc.*, 1984, **106**, 8146.
- 15 V. Barone, F. Lelj, A. Bavoso, B. Di Blasio, P. Grimaldi, V. Pavone and C. Pedone, *Biopolymers*, 1985, **24**, 1759.
- 16 G. M. Bonora, C. Toniolo, B. Di Blasio, V. Pavone, C. Pedone, E. Benedetti, I. Lingham and P. Hardy, *J. Am. Chem. Soc.*, 1984, **106**, 8152.
- 17 C. Toniolo, G. M. Bonora, A. Bavoso, E. Benedetti, B. Di Blasio, V. Pavone, C. Pedone, V. Barone, F. Lelj, M. T. Leplawy, K. Kaezmarek and A. Redlinski, *Biopolymers*, 1988, **27**, 373.
- 18 B. Di Blasio, V. Pavone, C. Isernia, C. Pedone, E. Benedetti, C. Toniolo, P. M. Hardy and I. Lingham, *J. Chem. Soc., Perkin Trans. 2*, 1992, 523.
- 19 S. Prasad, R. B. Rao and P. Balam, *Biopolymers*, 1995, **35**, 11.
- 20 J. Karle and I. L. Karle, *Acta Crystallogr.*, 1966, **21**, 849.
- 21 E. Egert and G. M. Sheldrick, *Acta Crystallogr., Sect. A.*, 1988, **41**, 262.
- 22 J. Karle, *Acta Crystallogr.*, 1968, **24**, 182.
- 23 I. L. Karle, J. L. Flippen-Anderson, K. Uma and P. Balam, *Int. J. Peptide Protein Res.*, 1988, **32**, 536.
- 24 S. Datta, N. Shamala, A. Banerjee and P. Balam, *Int. J. Peptide Protein Res.*, in press.
- 25 E. N. Baker and R. E. Hubbard, *Progr. Biophys. Mol. Biol.*, 1984, **44**, 97.
- 26 I. L. Karle, J. L. Flippen-Anderson, K. Uma and P. Balam, *Biopolymers*, 1990, **29**, 1835.
- 27 I. L. Karle, R. B. Rao, R. Kaul, S. Prasad and P. Balam, *Biopolymers*, 1996, **39**, 75.
- 28 I. L. Karle, R. Kaul, R. B. Rao, S. Raghothama and P. Balam, submitted for publication in *J. Am. Chem. Soc.*
- 29 IUPAC-IUB Commission on Biochemical Nomenclature, *Eur. J. Biochem.*, 1970, **17**, 193.

Paper 7/02109G
Received 26th March 1997
Accepted 29th May 1997